Slow light in photonic crystals

Slow light with a remarkably low group velocity is a promising solution for buffering and time-domain processing of optical signals. It also offers the possibility for spatial compression of optical energy and the enhancement of linear and nonlinear optical effects. Photonic-crystal devices are especially attractive for generating slow light, as they are compatible with on-chip integration and room-temperature operation, and can offer wide-bandwidth and dispersion-free propagation. Here the background theory, recent experimental demonstrations and progress towards tunable slow-light structures based on photonic-band engineering are reviewed. Practical issues related to real devices and their applications are also discussed.

TOSHIHIKO BABA[1,2]

[1]Department of Electrical and Computer Engineering, Yokohama National University, 79-5 Tokiwadai, Hodogaya-ku, Yokohama 240-8501, Japan
[2]CREST, Japan Science and Technology Agency, 5 Sanban-cho, Chiyoda-ku, Tokyo 102-0075, Japan

*e-mail: baba@ynu.ac.jp

The velocity of light in vacuum, c, is approximately 3×10^8 m s^{-1}, fast enough to make 7.5 round-the-world trips in a single second, and to move a distance of 300 mm in 1 ns. This ultrahigh speed is advantageous for efficient data transmission between two points, whether they are separated on a global scale or on a single chip; however, it also makes control of optical signals in the time domain difficult. Slow light is a technology now being investigated as a means to overcome this problem.

In next-generation information networks, path switching of optical packets at network nodes will become very important, and solutions that can perform the task with a high data rate, high throughput, and low power consumption are required. Engineers are now developing photonic routers that exploit all-optical processing to avoid the optical–electronic conversion that introduces a lot of inefficiency. Here, a key device is the optical buffer, a device that temporarily stores and adjusts the timing of optical packets. At present, solutions are based on mechanical variable delay lines and a combination of different delay lines with an optical switch, but these approaches are not ideal owing to their slow response. If the velocity of slow light can be controlled with a response speed much faster than the mechanical method, it could be a solution not only for buffering but also various types of time-domain processing, such as retiming, multiplexing and performing convolution integrals. Control over slow light could also improve the phase control in interferometric modulators and phased-array beam shapers. In addition, slow light offers the opportunity for compressing optical signals and optical energy in space, which reduces the device footprint and enhances light–matter interactions. With enhanced optical gain, absorption and nonlinearities per unit length, numerous optical devices, such as lasers, amplifiers, detectors, absorption modulators and wavelength converters, could be miniaturized.

The definition of velocity that is most meaningful in slow-light applications is the group velocity v_g, which describes the speed at which a pulse envelope propagates. In general, v_g is greatly reduced by a large first-order dispersion arising from an optical resonance within the material or structure. Initially, slow light was generated using extremely strong material dispersion; however, this review discusses dispersion arising from engineered structures, in particular photonic-crystal (PC) waveguides, which offer a promising approach for the on-chip integration of slow-light devices.

Photonic crystals are multidimensional periodic structures with a period of the order of the optical wavelength, λ. The research field became active in the late 1970s and 1980s (refs 1–3) with the development of photonic band theory, an optical analogue of electronic band theory, which can be used to compute the dispersion characteristics of light in arbitrary PC structures. The theory predicted the existence of a photonic bandgap (PBG), a frequency band of inhibited optical modes. Since the 1990s, PCs with PBGs have been explored for various device applications[4–12]. At present, PC slabs, a high-index thin film with a two-dimensional array of air holes surrounded by air cladding, are widely used because of their intrinsic lossless optical confinement and simple fabrication process. The PC waveguide (PCW) consists of a line defect of missing air holes in the PC slab[13–23]. Light propagates through the defect, confined by total internal reflection in the vertical direction and Bragg reflection, due to the PBG, in the lateral direction. It has been known since 2001 that the strong dispersion in this waveguide generates slow light in the vicinity of the photonic band edge[24–35].

When discussing a low v_g in a PCW, two important optical properties need to be considered: the frequency bandwidth of the effect and higher-order dispersion[36]. A fundamental limit to the first of these is the delay–bandwidth product (DBP), which affects all approaches to slow light[37–39]. Although a wide bandwidth is desirable in most applications, it often comes at the price of less delay. The DBP means that the extent to which the group velocity of light is reduced must be balanced with the required bandwidth for the application in mind. Regarding the second issue, the higher–order dispersion that usually occurs in simple slow-light PCWs severely distorts optical signals. This distortion can be eliminated either by combining two PCWs with opposite dispersion characteristics[36,40–45], using so-called dispersion-compensated slow-light devices, or by suppressing the higher-order dispersion using so-called zero-dispersion slow-light devices, comprising modified PCWs (refs 46–52) or a coupled-resonator optical waveguide (CROW) based on PC cavities or microrings[53–62]. It is now possible to slow down short optical pulses using some of these approaches.

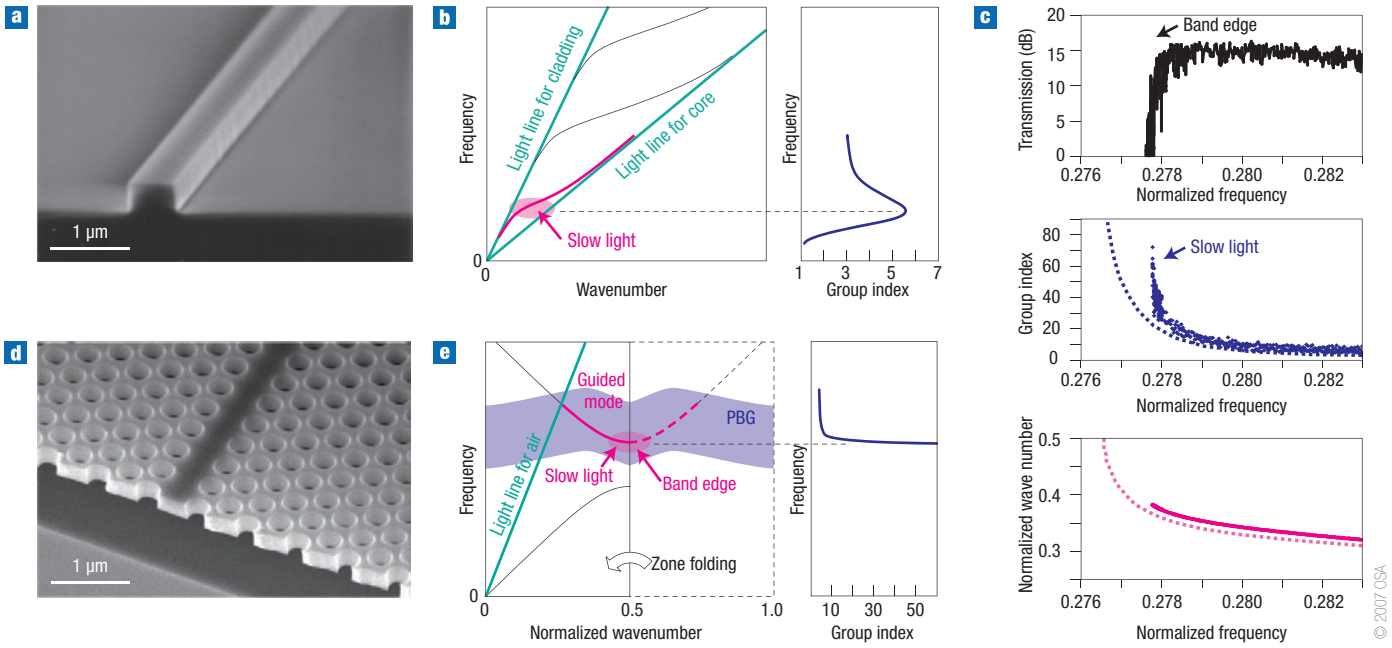

Figure 1 Waveguides, photonic bands and group-index characteristics. The normalized wavenumber means the wavenumber in units of reciprocal lattice $2\pi/a$, where a is the lattice constant. The normalized frequency is defined as $\omega a/2\pi c = a/\lambda$. **a**, Scanning electron microscope image and, **b**, schematic band diagram and group-index spectrum for a silicon PWW. **c**, Transmission spectrum, group-index spectrum and band diagram with respect to the normalized frequency for a silicon PCW. For the group-index spectrum and band diagram, dots denote experimental results obtained by the modulation phase-shift method, whereas dotted lines denote calculated results with an effective-index approximation. Adapted with permission from ref. 50. **d**, Scanning electron microscope image and, **e**, schematic band and group-index spectrum of a silicon PCW with respect to the absolute frequency.

Once it is possible to generate wideband dispersion-free slow light, the next important consideration is tunability. A variable v_g and delay were first demonstrated for band-edge slow light by externally controlling the material index of a PCW, although its bandwidth and tuning range were limited[29]. Later, tunability was also achieved using wideband dispersion-compensated slow light, and a visible time shift of optical pulses was observed by engineering the device structure and material index control[45].

Dynamic tuning of slow light, meaning that the tuning is performed while light is present in a device, is often advantageous, as it provides additional unique functions, such as frequency conversion and the complete stopping of light in PC devices and microrings[63–69]. Note, however, that the delay of slow light and the potential to stop light altogether is limited in practice by the lifetime of light, which is dominated by intrinsic and extrinsic losses. In PCWs, extrinsic losses need to be conquered to construct feasible optical buffers[23,70–73]. In contrast to the demanding requirements for buffers, the enhancement of optical and optoelectronic effects is simpler to achieve, as a reduction in v_g has already been shown to be beneficial for the miniaturization and improvement of light-control devices[52,74–85].

This review first presents a simple theoretical background of slow light for the better understanding of subsequent sections. It then focuses on the generation of useful slow light in PCW-based devices. Finally, some of the concepts already introduced are explained in detail and recent studies are reviewed.

SLOW-LIGHT THEORY AND THE DELAY–BANDWIDTH PRODUCT

The group velocity of light is given by the inverse of the first-order dispersion $(\mathrm{d}k/\mathrm{d}\omega)^{-1}$, where k and ω are the wavenumber and angular frequency, respectively[86]. The group index $n_g \equiv c/v_g = c(\mathrm{d}k/\mathrm{d}\omega)$ is regarded as a slow-down factor from the velocity, c. Note that, in any material, the material index itself is neither very large nor easy to modify; it can be changed by no more than several per cent by any form of external stimulation. Still, n_g is greatly enhanced in materials or structures with large first-order dispersion.

A notable example of a system that exhibits strong material dispersion is electromagnetically induced transparency (EIT) in a vapour or a solid at, in most cases, cryogenic temperatures[87–89]. It is a phenomenon that arises from the coherent resonance of light with photo-excited atoms and gives rise to a huge n_g (the maximum value is of the order of 10^{10}). In most cases, however, EIT responds only to slowly varying optical signals because the frequency window for optical transparency is usually very narrow (of the order of kilohertz at the maximum n_g). When a short optical pulse is incident on an EIT medium, it does not appear to be slowed, but instead resonant frequency components are filtered out, resulting in the smoothing and expanding (reshaping) of the optical pulse. A similar situation can be seen in optical resonators. In general, resonators exhibit strong structural dispersion at each resonant frequency. They form standing waves, which can be regarded as a sort of stopped light. As with EIT, resonators do not maintain the shape of the waveform of a short optical pulse.

Slow light has been observed in various media, but to be useful it needs to be achieved over a wide bandwidth. Detailed analysis of the DBP has been reported in numerous papers[37–39]; a simple treatment is shown here. Let us denote the material index or the modal equivalent index as n. Using the relation $k = \omega/(c/n)$,

$$n_g = c\frac{\mathrm{d}k}{\mathrm{d}\omega} = \frac{\mathrm{d}(n\omega)}{\mathrm{d}\omega} = n + \omega\frac{\mathrm{d}n}{\mathrm{d}\omega} \qquad (1)$$

When n_g is much greater than n, the DBP and its normalized form are given by

$$\Delta t\Delta f \cong \frac{L\Delta n}{\lambda} \qquad \text{and} \qquad n_g\left(\frac{\Delta f}{f}\right) \cong \Delta n \tag{2}$$

respectively, where Δt is the delay of light at a wavelength λ over a propagation length of L, Δf is the frequency bandwidth centred at a frequency of $f = \omega/2\pi$, and Δn is the change of n in the bandwidth. The time duration of one optical bit is approximately given by Δf^{-1}, although an accurate value depends on the modulation format. Therefore, the DBP $\Delta t\Delta f$ is a good indication of the highest buffering capacity that the slow-light device potentially provides. On the other hand, the normalized form can be more useful when devices that have different lengths and different operating frequencies are compared. The shortest spatial length of one bit ΔL is approximated by

$$\Delta L \approx \lambda/\Delta n \tag{3}$$

Equations (2) and (3) indicate that Δn is the dominant factor for achieving a large buffering capacity. In materials and structures that have low dispersion, Δn changes linearly with Δf when Δf is much greater than f. On the other hand, Δn can be maximized in highly dispersive media independently of Δf by optimizing photo-excitation and structural design, for example, and, according to equation (2), a large n_g and long Δt are obtained by narrowing Δf. The maximum value of Δn is usually smaller than 1.0. Taking, for example, a case where $\Delta n = 0.1$ and $\Delta f = 40$ GHz (or 40 kHz) at $\lambda = 1.55$ μm, then $n_g = 485$ (or 4.85×10^8), $\Delta t = 1.6$ μs (1.6 s), $\Delta t\Delta f = 64{,}000$ (64,000) and $\Delta L = 15.5$ μm are expected for $L = 1$ m. This shows the feasibility of constructing a slow-light-based optical buffer for a small number of packets, although such a long L is not ideal for on-chip integration.

SLOW LIGHT IN HIGHLY DISPERSIVE STRUCTURES

For the on-chip integration and room-temperature operation of slow-light devices, highly dispersive structures are more advantageous than dispersive materials (see Fig. 1). To my knowledge, the device with which slow light was first observed in 2001 was a silicon photonic-wire waveguide[90] (PWW), which is widely used in silicon photonic devices[91,92]. It is a simple rectangular channel waveguide with a high index contrast between the silicon core and air or SiO_2 cladding (Fig. 1a). The propagation loss of this waveguide is sometimes measured from the finesse of the internal Fabry–Pérot resonance. In the first observation, the group index n_g was evaluated from the relation $n_g = \lambda^2/2L\Delta\lambda_r$ ($\Delta\lambda_r$ is the peak spacing of the resonances) as around four to five. This was not caused by the resonance but by the large dispersion arising from the high index contrast, which largely changes the propagation constant (k in the propagation direction) with respect to ω, particularly near the cut-off of the waveguide mode[90,93] (Fig. 1b). This result suggests that the dispersion term in equation (1) can be comparable to or larger than n itself even in a simple waveguide. After this experiment, much larger dispersion was reported with a PCW (ref. 25). Owing to zone-folding of the guided-mode band and the coupling of forward and backward propagating waves forming a standing wave, the first-order dispersion diverges to infinity, and slow light (or stopped light) occurs near (or at) a cut-off point called the band edge (Fig. 1d,e). Note that similar divergence occurs in any Bragg structure; however, Δn is typically smaller than 0.01 in shallow gratings and low-index-contrast multilayer stacks. Owing to the high index contrast of the PC slab, the band is strongly deformed near the band edge and a large Δn ranging from 0.1 to 1 is obtained.

A PCW is usually fabricated on a silicon-on-insulator (SOI) or III–V compound semiconductor substrate by using standard semiconductor processes, including high-resolution lithography, selective dry etching and wet etching. A typical structure consists of air holes with a diameter of 240 nm and a lattice constant of 450 nm for a target wavelength of $\lambda = 1.55$ μm. Present technology means that such structures, etched to a depth of around 200 nm, can be achieved with a disorder within several nanometres. To evaluate v_g of the slow light, the following three methods are used: (1) the frequency-domain interferometric method, which measures the spacing of the Fabry–Pérot resonances[90,25] or Mach–Zehnder interference (MZI) peaks[29]; (2) the time-domain modulation phase-shift method, which detects the phase of light sinusoidally modulated at gigahertz frequencies[20,42–45,49,50,52]; and (3) time-domain direct observation of the short optical pulse transmission[26,27,30,31,44,45,50,52]. A rapid increase in n_g from less than ten to several tens or several hundreds is observed near the band edge using the first two methods (Fig. 1c). For the simple PCW, the third method is not easily applied because of severe higher-order dispersion. Scanning near-field optical microscopy has revealed pulse broadening by capturing snapshots of the propagating pulse, where the slow-light part has been left behind by the fast-light parts[30]. The major component of the higher-order dispersion is the group-velocity dispersion (GVD), given by $d(v_g^{-1})/d\omega = d^2k/d\omega^2$. It usually becomes extremely large near the band edge; a typical GVD constant is of the order of 100 ps nm^{-1} mm^{-1}, which

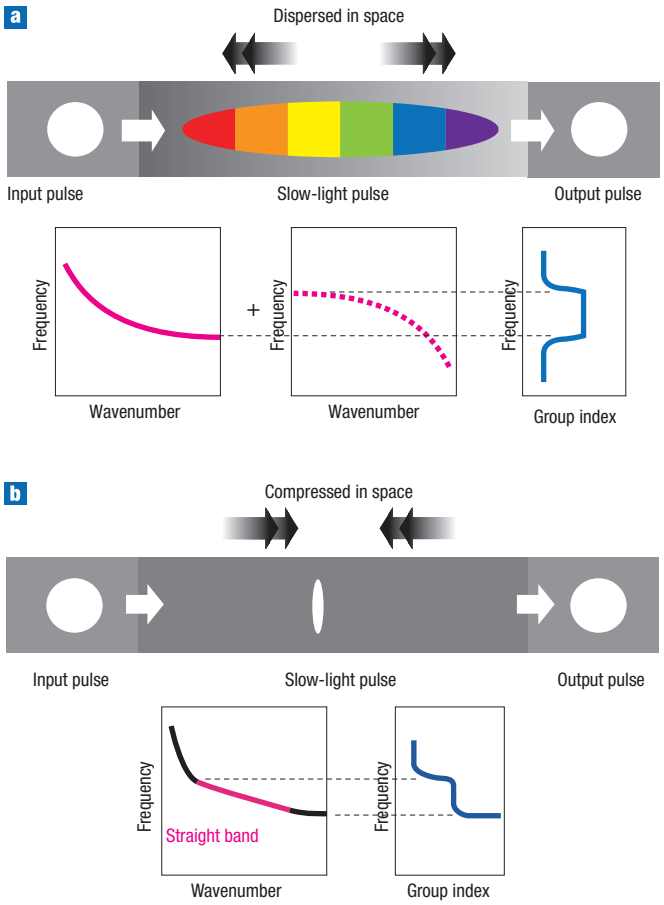

Figure 2 Schematic operation, band diagrams and group-index spectra of dispersion-free slow-light devices. **a**, Dispersion-compensated slow-light device with chirped structure. **b**, Zero-dispersion slow-light device. **a**,**b**, Upper panels illustrate the condition of slow-light pulses in the device, and the lower panels give the corresponding band diagram (left) and group-index spectrum (right).

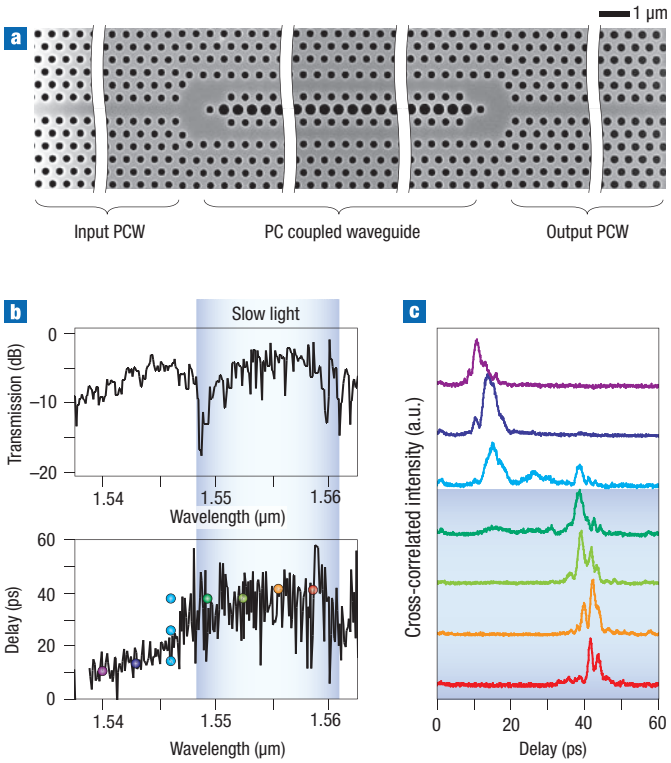

Figure 3 A PC coupled waveguide and its light-propagation characteristics. **a**, A scanning electron microscope image of a fabricated device on an SOI substrate. **b**, Measured transmission and delay spectra. The pale-blue region indicates wideband dispersion-compensated slow light. Fine oscillation is caused by the internal resonance. Plotted circles correspond to the pulse delay observed in **c**. **c**, Cross-correlation trace of the optical pulse at each central wavelength denoted by the colour of the circles plotted in **b**. Adapted with permission from ref. 45.

is 10^6 times larger than that of single-mode silica fibres. Because of this, dispersion-compensated and zero-dispersion slow light are very important (Fig. 2). Even though a high buffering capacity is potentially expected from a large DBP in a PCW device specifically designed for wideband slow light, the net capacity is finally determined by how the GVD is suppressed.

DISPERSION-COMPENSATED SLOW LIGHT

Photonic-band analysis can be used to design a device such that a positive or negative GVD in the first part of the device is cancelled out by an opposite GVD in the second part. For example, a line defect filled with air holes offset by half a period[94] can create a waveguide with the opposite GVD to that of the simple PCW. These two different waveguides can be coupled together using a chirped structure[36] in which some structural parameters are gradually changed along the length of the waveguides so that the guided-mode band is smoothly shifted[28]. Each wavelength component of light incident on the first waveguide reaches a corresponding band-edge position in the chirped structure. Band edges of these waveguides are set to always be the same in the chirped structure. Therefore, conserving ω and k, light is coupled to the second waveguide and simultaneously delayed near the band edges. Finally, the light propagates along and exits the second waveguide; hence, GVD of slow light is well suppressed over a wide bandwidth determined by the chirped range (completely eliminated at the central frequency). A technical problem of this device is that a small fluctuation in the band-edge matching causes a strong oscillation in the transmission spectrum. The other option in device design is to cascade two PCWs (ref. 41) where the GVD in the first part is simply compensated by the opposite GVD in the second part. In this case, the connection loss is an issue because modal profiles of these PCWs are completely different particularly near the band edge. Adiabatic tapers can reduce the loss, but then the structure usually becomes long for a compact slow-light device.

A more sophisticated device based on a similar approach, but free from the matching and connection issues is the chirped PC coupled waveguide[42] (Fig. 3a). It consists of two parallel PCWs whose adjacent air holes are partially enlarged or shifted to mould the band shape[95]. It maintains even and odd symmetric modes; the even symmetric mode shows a flat band with an inflection point that is sandwiched by the opposite GVD characteristics. This mode can be selectively used by connecting it with input/output waveguides through a symmetric branch, and confluence. With a chirped structure, the slow-light condition at the flat band is appropriately broadened. A simple theoretical consideration indicates that the DBP in equation (2) is still valid in the chirped structure by replacing n_g with its average value. In a device where $L = 250$ μm fabricated on an SOI substrate, a $\Delta t \sim 40$ ps and $n_g = 40$–60 were experimentally measured with a wavelength bandwidth of 10–12 nm at $\lambda \sim 1.55$ μm ($\Delta f = 1.2$–1.4 THz, $\Delta f/f \sim 0.7\%$, refs 44,45). The GVD compensation in the device was confirmed from a pulse transmission experiment. Subpicosecond optical pulses were maintained at the output with some amount of dispersion even in the slow-light band (Fig. 3b,c). The maximum DBP evaluated was 57 and the corresponding Δn was 0.35, which approximately agrees with the expectation from equation (2), but the net buffering capacity was limited to 12 bit as a result of the imperfect dispersion compensation. A DBP of 1,000 would be obtained by lengthening the device to 5 mm. But to achieve a net capacity of 1 kbit, the disorder in the fabricated device must be reduced and the third- and higher-order dispersion[33,59] must be suppressed by further engineering the structure and band.

In these devices, incident optical pulses are initially spatially dispersed and then recovered in the GVD compensation process (Fig. 2a). Therefore, it is effective for suppressing optical nonlinearity caused by the high intensity of the slow light.

ZERO-DISPERSION SLOW LIGHT

In fibre optics, the term 'zero dispersion' is usually used for zero GVD. But if the simple PCW is modified so as to give a straight guided-mode band, any higher-order dispersion components are also eliminated. Although the band cannot actually be completely straight, such dispersion components can be effectively reduced by this approach. In contrast to dispersion-compensated slow light, the pulse shape is compressed in space and accordingly its internal intensity is enhanced (Fig. 2b). Therefore, the approach is effective for the enhancement of optical nonlinearities.

There are a variety of ways to optimize the structure of a device to obtain a straight band. A PCW can be modified for this purpose by reducing the diameter of the innermost air holes adjacent to the line defect and increasing the diameter of the other air holes (Fig. 4a)[50]. This brings the guided-mode and slab-mode bands closer together and gives rise to their anticrossing. When this behaviour is appropriately controlled, the guided-mode band is straightened. It results in a step-like increase in n_g near the band edge and a nearly flat spectrum of n_g at the step. Fine tuning of the two air-hole diameters balances n_g and the bandwidth. This type of slow light has been observed experimentally: values of $\Delta t = 40$–50 ps and $n_g = 30$–37 were evaluated for a wavelength bandwidth of 11–5 nm, respectively, for $L = 400$ μm at $\lambda \sim 1.55$ μm (Fig. 4b). The corresponding DBP is 56 and $\Delta n = 0.21$. The transmission of subpicosecond optical pulses was also observed as evidence of the low higher-order dispersion[52].

A semi-straight band is also obtained at the centre of the transmission band of CROWs, where only the GVD is eliminated. The weak coupling between adjacent high-quality-factor microcavity resonators forms a band with a large n_g and a flat spectrum around the centre of its transmission window. Two adjacent PC nanocavities, each of which is created by shifting some of the air holes in the PC slab, exhibit two resonant peaks corresponding to coupled modes[96]. When 10–100 of such PC microcavities are lined up to form a CROW, a transmission band appears[62]. As light propagates along the CROW, localization at each cavity introduces a time delay. In this structure, the radiation loss is an intrinsic problem. Because the PC CROW has both the periodicity of the PC and the microcavities, the band is zone-folded, in addition to the original zone folding due to the PC. As a result, light is strongly diffracted, and the guided mode is easily coupled to free-radiation modes. This loss may be minimized by reducing the loss in each cavity and the coupling strength. Of course, CROWs do not necessarily involve a PC slab. Coupled microrings[59–61], microdisks[97,98] and microspheres[99–101] have also been studied as CROWs. In a 100-cascaded-microring structure (Fig. 5), an error-free delay of 220 ps was observed for signals of up to 4 Gbit s^{-1} (ref. 61). In these CROWs, a strong oscillation appears in the transmission spectrum owing to disordered or even uniform coupling between cavities. Therefore the transmission of short optical pulses is still a challenge. Another type of CROW is a multicavity dielectric stack, which can be regarded as a one-dimensional PC with multiperiodicity[58]. In this structure, the radiation loss is avoided by expanding the incident optical beam, and the transmission spectrum is flattened by apodizing the layer thicknesses.

TUNABILITY

Tuning of n_g is achieved by changing the material or modal equivalent index, or both. To differentiate from dynamic tuning, which is discussed in the next section, it is assumed here that the tuning is performed before the light enters the device.

The simplest way of tuning is to use the band-edge shift associated with a uniform Δn. With a small Δn, the guided-mode band of the PCW simply shifts, almost maintaining its shape, and n_g at frequencies slightly higher than the band edge changes sharply. Thermal heating and carrier injection are often exploited to change the refractive index of the PC slab. Heating allows a large Δn of up to approximately 1%, and n_g was actually tuned in the range of 20–60 using a heater integrated with a PCW on an SOI substrate[29]. Owing to quick thermal diffusion in the small device, its response time was 100 ns. The band-edge shift simultaneously changes k leading to a large phase shift of light in the device, and this was observed in an MZI switch with a short device length of 160 μm (ref. 81). A much faster response is expected by using carrier plasma effects for carrier injection. The response time depends on the carrier recombination lifetime and diffusion and can be shorter than 1 ns (ref. 102), which is sufficient for optical packet buffers. In this case, Δn has a maximum of about 0.1% resulting in a narrow tuning range.

It is important that tuning should be performed for GVD-free slow light. A change of n_g in GVD-free slow light is not obtainable by the band-edge shift approach, but requires the change of the first-order dispersion at the frequency of the incident light. Regarding dispersion-compensated slow light, this was achieved by engineering a sloping Δn in addition to the structural chirping[45]; when the PC coupled waveguide was heated so that the temperature slope was formed, the delay of pulses with a duration of 0.9 ps was tuned to as long as 23 ps, with an average output pulse duration of 3.3 ps, and for pulses with a duration of 1.2 ps the delay was tuned to as long as 8 ps (Fig. 6). For zero-dispersion slow light, the slope of the straight band must be directly changed, which may require a complicated localized change of n. However, an additional advantage here is that the simple shift of the straight band with the uniform Δn gives a large phase change in the device, keeping the same group velocity, thus improving the performance of MZI modulators and switches.

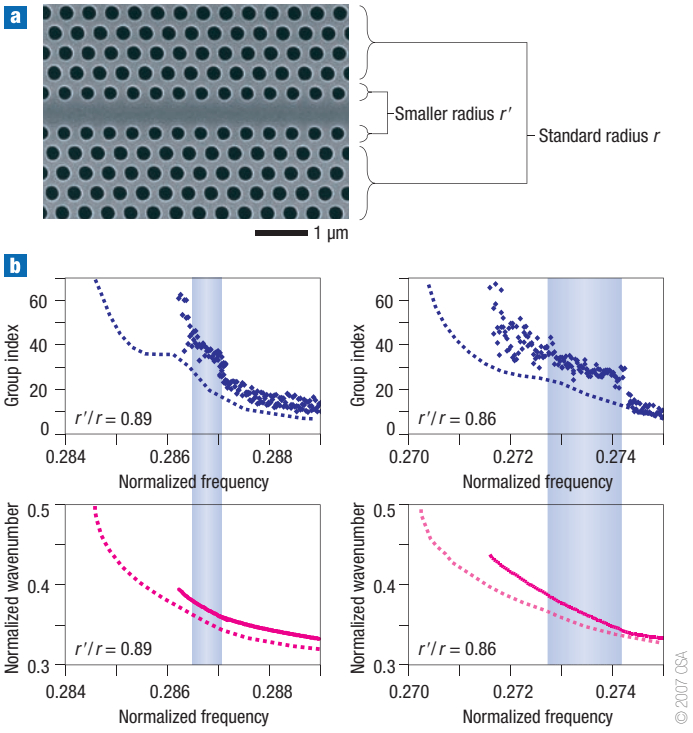

Figure 4 A PCW modified for zero-dispersion slow light. **a**, A scanning electron microscope image of the top of a fabricated device on an SOI substrate. **b**, The group index and band structure for two ratios of air-hole radius. Details are the same as those in Fig. 1d. The pale-blue region indicating the step-like increase in group index shows the low-dispersion slow light. Adapted with permission from ref. 50.

DYNAMIC TUNING FOR THE STOPPING OF LIGHT

Thus far, slow light has been thought of in terms of an invariant frequency spectrum that does not change within the device. If wideband optical signals are converted into a very narrow spectrum, n_g can be freely enhanced, according to equation (2). In the extreme case that Δf approaches zero, n_g diverges and the light is completely stopped. Strictly speaking, light does not stop; its back and forth motion forms a standing wave, storing optical energy, and it just appears to be stopped. But the DBP no longer represents a constraint for such light if the information carried by the signals is not lost during the process. The information is actually stored in the spatial distribution of light, as k is conserved. Such an operation is achievable by dynamic tuning, which is a type of parametric tuning process[66]. As observed in interferometric modulators, a temporal change of n leads to a phase and frequency shift of light passing through the material. Suppose that n in a waveguide is changed quickly and adiabatically within the time that optical signals are still present in the waveguide. In this situation, the wavelength (frequency) of light is changed in (inverse) proportion to n, while almost maintaining the spatial distribution. If the waveguide is designed so that n_g diverges with an increase Δn, then the signal bandwidth is compressed into a single frequency by the dynamic tuning, and the light is simultaneously stopped. A structure that has been theoretically discussed is a system consisting of a PCW coupled with an adjacent series of PC cavities, which can, in total,

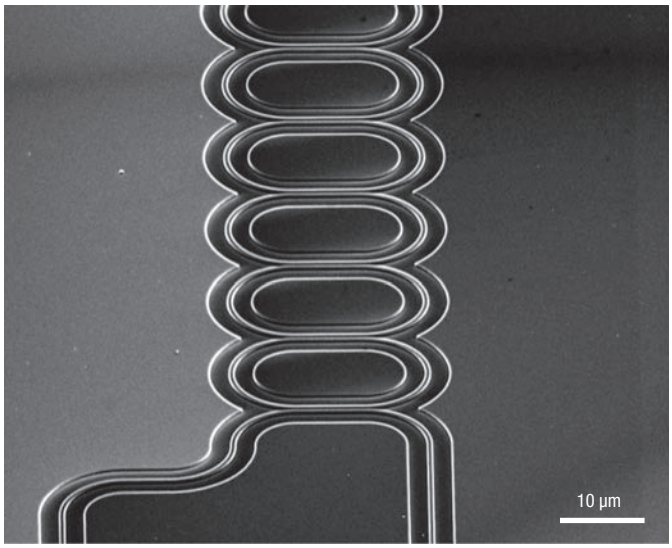

Figure 5 A CROW consisting of cascaded microrings fabricated on an SOI substrate. Multiple microrings are evanescently coupled with each other and the end microring is coupled with an access waveguide on the near side[61].

be regarded as a CROW (ref. 64). In this case, the coupling strength is controlled by a local Δn, so that n_g in the system is increased. It is equivalent to the dynamic increase in the quality factor of each cavity, so light propagating in the PCW is caught in the cavities. If long and complicated optical signals are present in the device during the tuning, they are divided into pieces and the envelope distribution is transcribed into the series of cavities. A reverse process, which eliminates Δn, faithfully recovers the initial light propagation. Experimentally such dynamic tuning has been demonstrated for a single optical pulse in a coupled system comprising a PCW and a PC single cavity with a phase shifter[68] and a system comprising a PWW and a couple of microrings[69]. The coupling condition was controlled using the carrier plasma effect, and the temporal catch and release of a pulse was demonstrated. Regarding the PWW–microring structure, a variable transmission spectrum similar to that in EIT was also studied[103,104].

A drawback of the dynamic tuning, compared with simple slow light, is the large device footprint needed for storing a series of optical signals. The envelope distribution of the optical signals is not compressed in space during the dynamic tuning but just stopped as it is. The number of signals stored in the device is limited to 400 for $L = 1$ m, $n = 3$ and $\Delta f = 40$ GHz. This constraint could be relaxed by the pre-compression of light in a slow-light device before the dynamic tuning[63–65]. Another constraint is that once the dynamic tuning is performed, subsequent signals cannot be input to the device until the reverse process is completed. Therefore, this process is suitable for optical RAM (random access memory) operation.

EXTRINSIC LOSS

In a well designed PCW, the guided-mode band is ideally lossless as a result of the optical confinement by the PBG in the lateral direction and by the total internal reflection in the vertical direction. In fact, however, the light scattering owing to structural disorder and material absorption give rise to a loss. As estimated above, buffering on the microsecond timescale requires a device length of $L = 1$ m, even for slow light. The total loss must be within a range that can be recovered by the gain of a standard optical amplifier, for example, less than 20 dB in the worst case. The waveguide loss should be lower than 0.2 dB cm^{-1} in the slow-light regime.

The reduction in scattering loss is, in some senses, the most crucial problem. The scattering loss in conventional index-confinement waveguides depends approximately on $\Delta^{2.5}$, where $\Delta \equiv (n_1^2 - n_2^2)/2n_1^2$ is the relative refractive-index difference between the core index n_1 and cladding index n_2 (ref. 105). Therefore, the loss in high-index-contrast waveguides, such as silicon PWWs, where Δ is more than 40%, can be a factor of 10^4–10^5 higher than that of conventional silica-based waveguides where Δ is less than 0.5%. Nevertheless, the loss in a PWW has been reduced to around 1 dB cm^{-1} by recent technical improvements[106–108]. The loss in the PCW on an SOI substrate, which has the same Δ, is expected to be lower because the scattering of the guided mode into radiation modes could be suppressed by the PBG (ref. 18). However, losses measured so far are still higher. In addition, low loss is limited to the low-n_g regime; much larger losses are observed near the band edge. There are active discussions about the dependence of loss on n_g. Some experimental results suggest n_g^2 and $\sqrt{n_g}$ dependences, which are attributed to doubly enhanced back-scattering and the change in modal profile respectively[23,73]. This must be further investigated to suppress the loss in a practical design.

The interband absorption should be negligible when the material bandgap, E_g, is larger than the photon energy. But the absorption extends to longer wavelengths in indirect-bandgap materials such as silicon. Also, absorption centres could be introduced into the top silicon layer of commercially available SOI wafers during fabrication. In addition, nonlinear two-photon absorption in silicon will be a problem at $\lambda \sim 1.55$ μm; it scales up with n_g^2. Once two-photon absorption occurs, excited carriers lead to self-phase modulation and free-carrier absorption. This has been observed in silicon PWWs when the waveguide is a millimetre to a centimetre long and the incident power reaches the order of a watt[109–112]. These effects can occur for a much lower power and in a much shorter waveguide with a large n_g for slow light. Actually, they were observed for picosecond optical pulses in a zero-dispersion slow-light PCW with a power of 0.15 W and an effective slow-light length of 300 μm (ref. 52). To completely suppress two-photon absorption, a material with E_g larger than twice the photon energy at $\lambda \sim 1.55$ μm is desired for the PC slab[113].

An additional loss associated with slow light occurs in the coupling between slow-light devices and input/output devices. When these devices are connected directly, slow light with an exotic modal profile is strongly reflected or scattered, or both. Some adiabatic structures are effective for the transformation of the modal profile between a PWW and a PCW (refs 114–117). Also, almost negligible reflection, less than −30 dB, is calculated for the chirped PC coupled waveguide, in which the incident light is gradually transformed into slow light[42].

ENHANCED LIGHT–MATTER INTERACTION

In lasers, amplifiers and absorption modulators, gain and absorption coefficients per unit length increase linearly with n_g when they are constant per unit time. As mentioned above, resonators can be thought of as light-stopping devices at certain frequencies. In PCs fabricated with III–V materials, laser operation occurs at band edges[118–122]. This is usually explained as a distributed-feedback (DFB) effect, but can also be treated as a slow-light effect. Let us consider a PCW laser[123–125] perfectly open to free space, as an example. The photon lifetime in this waveguide is equivalent to the time for light propagation, and it is extended with n_g, so light acquires sufficient gain for laser operation. In practice, some reflection occurs at the waveguide ends, and this determines the phase and wavelength of the resonance. Consequently, the lasing wavelengths are not

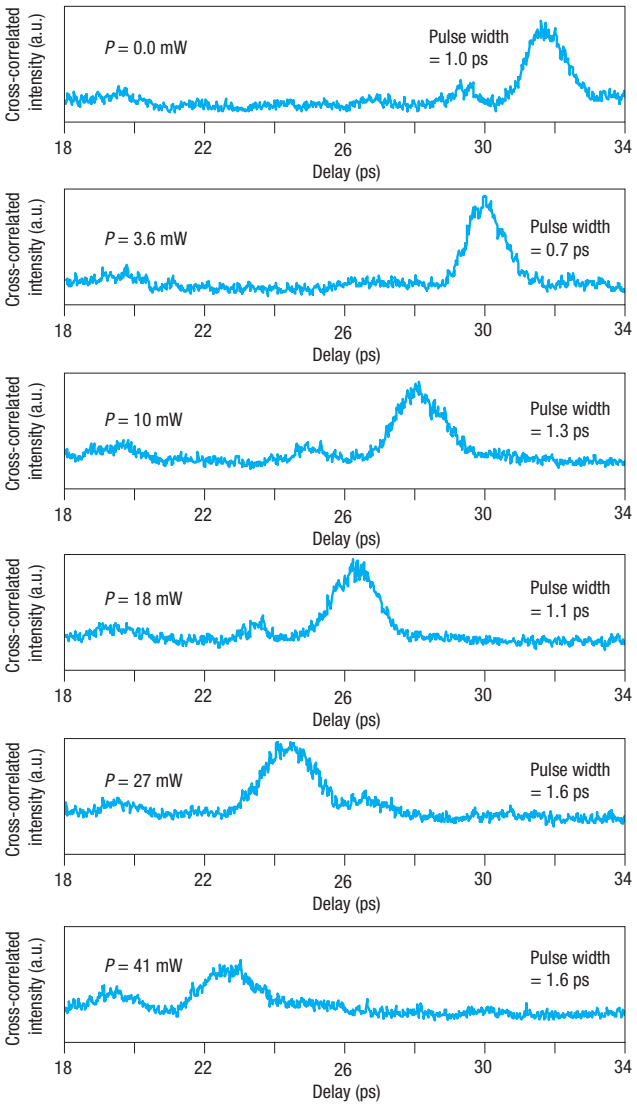

Figure 6 Delay tuning of slow-light pulses in a chirped PC coupled waveguide. Subpicosecond optical pulses were incident on the device. Wideband dispersion-compensated slow light is obtained by chirping the air-hole diameter of the device, that is, by increasing the air-hole diameter of the device gradually along the light-propagation direction. The delay was externally controlled by laser heating with power *P*, which formed the slope of the temperature and corresponding material index, and changed the effective amount of chirping. Here, the pulse width is evaluated by deconvoluting the reference pulse from the cross-correlation trace. Adapted with permission from ref. 45.

precisely aligned with the band edge, but are slightly shifted into the waveguide band. Just as happens in the transmission spectrum of the passive PCW, the photo-pumped lasing spectrum in a GaInAsP PCW exhibits a narrowing of the Fabry–Pérot modal spacing towards the band edge[124].

The enhanced gain and absorption are expected to reduce the size of semiconductor optical amplifiers[83] (SOAs) and electro-absorption modulators[85]. A simple theoretical estimation shows a high modal gain of 25 dB in a 10-μm-long GaInAsP SOA with $n_g = 100$ and an injection current of 3 mA. Owing to the small device size, reasonably low current level and severe thermal heating under continuous-wave conditions, an output power higher than 10 dBm would not be expected for such a small device, making it suitable as a pre-amplifier and a loss compensator in photonic circuits. A short electroabsorption modulator based on slow light was demonstrated using a vertical cavity with oblique incident light. A big challenge that remains in regard to these devices is the integration of electrical elements with a PCW. Photonic-crystal waveguides comprising an active layer and p- and n-type semiconductor cladding with perforated deep air holes have been studied to enable current injection and to apply a voltage.

Second- and third-order optical nonlinearities are also enhanced as n_g^2. Two-photon absorption, another propagation loss mechanism, can be used to create an optical limiter. Similarly, self-phase modulation, four-wave mixing, super-continuum generation, and Raman amplification have been observed in silicon PWWs (refs 109–113,126–131). Here, two-photon absorption and associated free-carrier absorption often become a problem because the waveguide channel is electronically isolated. The zero-dispersion slow-light PCW is expected to enhance not only two-photon absorption and self-phase modulation, but also other nonlinearities mentioned above. It should also decrease free-carrier absorption due to fast carrier diffusion with a lifetime of less than 1 ns, as it is electrically connected with other parts of the silicon layer.

SUMMARY

Slow light with a group velocity several tens to several hundreds of times lower than *c* is attainable with present PCW-based technology. This is an impressive result when considering the probable bandwidth requirements for future data traffic, above 40 GHz. The DBP will soon reach 100–1,000 by increasing the device length to the millimetre or centimetre scale and by reducing extrinsic losses. Dispersion management and tunability add greatly to the value of slow light. Owing to dispersion-compensated and zero-dispersion structures, slow propagation of subpicosecond optical pulses has been confirmed. Wide-range delay tuning has also been achieved for dispersion-compensated slow light. This unique functionality was previously only available in mechanically variable delay lines, with commercial devices offering a tuning response time on the millisecond timescale. The absolute value of the delay in PC devices is limited to less than 1 ns. The extrinsic loss, mainly due to light scattering, is the most crucial problem to be overcome and must be suppressed by further structure optimization and improvements to the fabrication process. Zero-dispersion slow-light pulses enable studies of enhanced light–matter interaction. In particular, the enhancement of optical nonlinearities has started to be observed experimentally, which is of great interest for adding complex functions in PC integrated circuits.

doi:10.1038/nphoton.2008.146

References

1. Ohtaka, K. Energy band of photons and low-energy photon diffraction. *Phys. Rev. B* **19,** 5057–5067 (1979).
2. Yablonovitch, E. Inhibited spontaneous emission in solid-state physics and electronics. *Phys. Rev. Lett.* **58,** 2059–2062 (1987).
3. John, S. Strong localization of photons in certain disordered dielectric superlattices. *Phys. Rev. Lett.* **58,** 2486–2489 (1987).
4. Bowden, C. M., Dowling, J. P. & Everitt, H. O. Special issue on development and applications of materials exhibiting photonic band gaps. *J. Opt. Soc. Am. B* **10,** 280–413 (1993).
5. Joannopoulos, J. D., Meade, R. D. & Winn, J. N. *Photonic Crystals– Moulding the Flow of Light* (Princeton Univ. Press, Princeton, 1995).
6. *Photonic Band Gap Materials* (ed. Soukoulis, C. M.) (Kluwer, Dordrecht, 1996).
9. Scherer, A., Doll, T., Yablonovitch, E., Everitt, H. O. & Higgins, J. A. Special issue on electromagnetic crystal structures, design, synthesis, and applications. *J. Lightwave Technol.* **17,** 1928–1930 (1999).
8. *Photonic Crystals and Light Localization in the 21st Century* (ed. Soukoulis, C. M.) (Kluwer, Dordrecht, 2001).
9. Krauss, T. K. & Baba, T. Feature section on photonic crystal structures and applications. *IEEE J. Quantum Electron.* **38,** 724–956 (2002).

10. *Roadmap on Photonic Crystals* (eds Noda, S. & Baba, T.) (Kluwer, Norwell, 2003).
11. *Photonic Crystals Physics, Fabrication and Applications* (eds Inoue, K. & Ohtaka, K.) (Springer, Berlin, 2004).
12. Joannopoulos, J. D., Johnson, S. G., Winn, J. N. & Meade, R. D. *Photonic Crystals—Moulding the Flow of Light* 2nd edn (Princeton Univ. Press, Princeton, 2008).
13. Baba, T., Fukaya, N. & Yonekura, J. Observation of light transmission in photonic crystal waveguides with bends. *Electron. Lett.* **35,** 654–655 (1999).
14. Loncar, M., Nedeljkovic, D., Doll, T., Vuckovic, J. & Scherer, A. Waveguiding in planar photonic crystals. *Appl. Phys. Lett.* **77,** 1937–1939 (2000).
15. Smith, C. J. M. *et al.* Low-loss channel waveguides with two-dimensional photonic crystal boundaries. *Appl. Phys. Lett.* **77,** 2813–2815 (2000).
16. Noda, S., Chutinan, A. & Imada, M. Trapping and emission of photons by a single defect in a photonic bandgap structure. *Nature* **407,** 608–610 (2000).
17. Notomi, M. *et al.* Singlemode transmission within photonic bandgap of width-varied single-line-defect photonic crystal waveguides on SOI substrates. *Electron. Lett.* **37,** 293–295 (2001).
18. Baba, T. *et al.* Light propagation characteristics of straight single line defect optical waveguides in a photonic crystal slab fabricated into a silicon-on-insulator substrate. *IEEE J. Quant. Electron.* **38,** 743–752 (2002).
19. Sugimoto, Y. *et al.* Low propagation loss of 0.76 dB/mm in GaAs-based single-line-defect two-dimensional photonic crystal slab waveguides up to 1 cm in length. *Opt. Express* **12,** 1090–1096 (2004).
20. Notomi, M. *et al.* Waveguides, resonators and their coupled elements in photonic crystal slabs. *Opt. Express* **12,** 1551–1561 (2004).
21. Bogaerts, W. *et al.* Nanophotonic waveguides in silicon-on-insulator fabricated with CMOS technology. *J. Lightwave Technol.* **23,** 401–412 (2005).
22. Dulkeith, E., McNab, S. J. & Vlasov, Y. A. Mapping the optical properties of slab-type two-dimensional photonic crystal waveguides. *Phys. Rev. B* **72,** 115102 (2005).
23. Kuramochi, E. *et al.* Disorder-induced scattering loss of line-defect waveguides in photonic crystal slabs. *Phys. Rev. B.* **72,** 161318 (2005).
24. Letartre, X. *et al.* Group velocity and propagation losses measurement in a single-line photonic-crystal waveguide on InP membranes. *Appl. Phys. Lett.* **79,** 2312–2314 (2001).
25. Notomi, M. *et al.* Extremely large group-velocity dispersion of line-defect waveguides in photonic crystal slabs. *Phys. Rev. Lett.* **87,** 253902 (2001).
26. Inoue, K. *et al.* Observation of small group velocity in two-dimensional AlGaAs-based photonic crystal slabs. *Phys. Rev. B* **65,** 121308 (2002).
27. Asano, T., Kiyota, K., Kumamoto, D., Song, B. S. & Noda, S. Time-domain measurement of picosecond light-pulse propagation in a two-dimensional photonic crystal-slab waveguide. *Appl. Phys. Lett.* **84,** 4690–4692 (2004).
28. Baba, T., Mori, D., Inoshita, K. & Kuroki, Y. Light localization in line defect photonic crystal waveguides. *IEEE J. Quant. Electron.* **10,** 484–491 (2004).
29. Vlasov, Y. A., O'Boyle, M., Hamann, H. F. & McNab, S. J. Active control of slow light on a chip with photonic crystal waveguides. *Nature* **438,** 65–69 (2005).
30. Gersen, H. *et al.* Real-space observation of ultraslow light in photonic crystal waveguides. *Phys. Rev. Lett.* **94,** 073903 (2005).
31. Finlayson, C. E. *et al.* Slow light and chromatic temporal dispersion in photonic crystal waveguides using femtosecond time of flight. *Phys. Rev. Lett.* **73,** 016619 (2006).
32. Engelen, R. J. P. *et al.* The effect of higher-order dispersion on slow light propagation in photonic crystal waveguides. *Opt. Express* **14,** 1658–1672 (2006).
33. Tanaka, Y. *et al.* Effect of third-order dispersion on subpicosecond pulse propagation in photonic-crystal waveguides. *Appl. Phys. Lett.* **89,** 131101 (2006).
34. Baba, T. & Mori, D. Slowlight engineering in photonic crystals. *J. Phys. D* **40,** 2659–2665 (2007).
35. Krauss, T. Slow light in photonic crystal waveguides. *J. Phys. D* **40,** 2666–2670 (2007).
36. Mori, D. & Baba, T. Dispersion-controlled optical group delay device by chirped photonic crystal waveguides. *Appl. Phys. Lett.* **85,** 1101–1103 (2004).
37. Tucker, R. S., Ku, P.-C. & Chang-Hasnain, C. J. Slow-light optical buffers – capabilities and fundamental limitations. *J. Lightwave Technol.* **23,** 4046–4066 (2005).
38. Khurgin, J. B. Optical buffers based on slow light in electromagnetically induced transparent media and coupled resonator structures: Comparative analysis. *J. Opt. Soc. Am. B* **22,** 1062–1074 (2005).
39. Miller, D. A. B. Fundamental limit to linear one-dimensional slow light structures. *Phys. Rev. Lett.* **99,** 203903 (2007).
40. Mori, D. & Baba, T. Wideband and low dispersion slow light by chirped photonic crystal coupled waveguide. *Opt. Express* **13,** 9398–9408 (2005).
41. Povinelli, M. L., Johnson, S. G. & Joannopoulos, J. D. Slow-light, band-edge waveguides for tunable time delays. *Opt. Express* **13,** 7145–7159 (2005).
42. Mori, D., Kubo, S., Sasaki, H. & Baba, T. Experimental demonstration of wideband dispersion-compensated slow light by a chirped photonic crystal directional coupler. *Opt. Express* **15,** 5264–5270 (2007).
43. Huang, S. C., Kato, M., Kuramochi, E., Lee, C. P. & Notomi, M. Time-domain and spectral-domain investigation of inflection-point slow-light modes in photonic crystal coupled waveguides. *Opt. Express* **15,** 3543–3549 (2007).
44. Kawasaki, T., Mori, D. & Baba, T. Experimental observation of slow light in photonic crystal coupled waveguides. *Opt. Express* **15,** 10274–10281 (2007).
45. Baba, T., Kawasaki, T., Sasaki, H., Adachi, J. & Mori, D. Large delay-bandwidth product and delay tuning of slow light pulse in photonic crystal coupled waveguide. *Opt. Express* **16,** 9245–9253 (2008).
46. Sakai, A., Kato, I., Mori, D. & Baba, T. Anomalous low group velocity and low dispersion in simple photonic crystal line defect waveguides. *Tech. Dig. IEEE/LEOS Annual Meet.* ThQ5 (Puerto Rico, IEEE/LEOS, 2004).
47. Petrov, A. Y. & Eich, M. Zero dispersion at small group velocities in photonic crystal waveguides. *Appl. Phys. Lett.* **85,** 4866–4868 (2004).
48. Settle, M. D. *et al.* Flatband slow light in photonic crystals featuring spatial pulse compression and terahertz bandwidth. *Opt. Express* **15,** 219–226 (2007).
49. Frandsen, L. H., Lavrinenko, A. V., Fage-Pedersen, J. & Borel, P. I. Photonic crystal waveguides with semislow light and tailored dispersion properties. *Opt. Lett.* **14,** 9444–9446 (2006).
50. Kubo, S., Mori, D. & Baba, T. Low-group-velocity and low-dispersion slow light in photonic crystal waveguides. *Opt. Lett.* **32,** 2981–2983 (2007).
51. Li, J., White, T. P., O'Faolain, L., Gomez-Iglesias, A. & Krauss, T. F. Systematic design of flat band slow light in photonic crystal waveguides. *Opt. Express* **16,** 6227–6232 (2008).
52. Hamachi, Y., Kubo, S. & Baba, T. Low dispersion slow light and nonlinearity enhancement in lattice-shifted photonic crystal waveguide. *Tech. Dig. Quantum Electron. Laser Sci. Conf.* QTuC1 (San Jose, OSA, 2008).
53. Yariv, A., Xu, Y., Lee, R. K. & Scherer, A. Coupled-resonator optical waveguide– A proposal and analysis. *Opt. Lett.* **24,** 711–713 (1999).
54. Oliver, S. *et al.* Miniband transmission in photonic crystal coupled resonator optical waveguide. *Opt. Lett.* **26,** 1019–1021 (2001).
55. Hosomi, K. & Katsuyama, T. A dispersion compensator using coupled defects in a photonic crystal. *IEEE J. Quant. Electron.* **38,** 825–829 (2002).
56. Martinez, A. *et al.* Group velocity and dispersion model of coupled-cavity waveguides in photonic crystals. *J. Opt. Soc. Am. A* **20,** 147–150 (2003).
57. Kim, W. J., Kuang, W. & O'Brien, J. D. Dispersion characteristics of photonic crystal coupled resonator optical waveguides. *Opt. Express* **25,** 3431–3437 (2003).
58. Fukamachi, T., Hosomi, K., Katsuyama, T. & Arakawa, Y. Group-delay properties of coupled-defect structures in photonic crystals. *Jpn J. Appl. Phys.* **43,** L449–L452 (2004).
59. Khurgin, J. B. Expanding the bandwidth of slow-light photonic devices based on coupled resonators. *Opt. Lett.* **30,** 513–515 (2005).
60. Poon, J. K., Zhu, L., De Rose, G. A. & Yariv, A. Transmission and group delay of microring coupled-resonator optical waveguides. *Opt. Lett.* **31,** 456–458 (2006).
61. Xia, F., Sekaric, L. & Vlasov, Y. Ultracompact optical buffers on a silicon chip. *Nature Photon.* **1,** 65–71 (2007).
62. Kuramochi, E., Tanabe, T., Taniyama, H., Kato, M. & Notomi, M. Observation of heavy photon state in ultrahigh-Q photonic crystal coupled resonator chain. *Tech. Dig. Quantum Phys. & Laser Sci. Conf.* QMG2 (Baltimore, OSA, 2007).
63. Yanik, M. F. & Fan, S. Stopping light all optically. *Phys. Rev. Lett.* **92,** 083901 (2004).
64. Yanik, M. F., Suh, W., Wang, Z. & Fan, S. Stopping light in a waveguide with an all-optical analog of electromagnetically induced transparency. *Phys. Rev. Lett.* **93,** 233903 (2004).
65. Khurgin, J. B. Adiabatically tunable optical delay lines and their performance limitations. *Opt. Lett.* **30,** 2778–2780 (2005).
66. Notomi, M. & Mitsugi, S. Wavelength conversion via dynamic refractive index tuning of a cavity. *Phys. Rev. A* **73,** 051803 (2006).
67. Preble, S. F., Xu, Q. & Lipson, M. Changing the colour of light in a silicon resonator. *Nature Photon.* **1,** 293–296 (2007).
68. Tanaka, Y. *et al.* Dynamic control of the Q factor in a photonic crystal nanocavity. *Nature Mater.* **6,** 862–865 (2007).
69. Xu, Q., Dong, P. & Lipson, M. Breaking the delay-bandwidth limit in a photonic structure. *Nature Phys.* **3,** 406–410 (2007).
70. Tanaka. Y. *et al.* Group velocity dependence of propagation losses in single-line-defect photonic crystal waveguides on GaAs membranes. *Electron. Lett.* **40,** 174–176 (2004).
71. Hughes, S. *et al.* Extrinsic optical scattering loss in photonic crystal waveguides—Role of fabrication disorder and photon group velocity. *Phys. Rev. Lett.* **94,** 033903 (2005).
72. Mookherjea, S. & Oh, A. Effect of disorder on slow light velocity in optical slow-wave structures. *Opt. Lett.* **32,** 289–291 (2007).
73. O'Faolain, L. *et al.* Dependence of extrinsic loss on group velocity in photonic crystal waveguides. *Opt. Express* **15,** 13129–13138 (2007).
74. Soljačić, M. *et al.* Photonic-crystal slow-light enhancement of nonlinear phase sensitivity. *J. Opt. Soc. Am. B* **19,** 2052–2059 (2002).
75. Konorov, S. O. *et al.* Coherent anti-Stokes Raman scattering of slow light in a hollow planar photonic band-gap waveguide. *Laser Phys.* **12,** 818–824 (2002).
76. Soljačić, M. *et al.* Nonlinear photonic crystal microdevices for optical integration. *Opt. Lett.* **28,** 637–639 (2003).
77. Soljačić, M. & Joannopoulos, J. D. Enhancement of nonlinear effects using photonic crystals. *Nature Mater.* **3,** 211–219 (2004).
78. Nakamura, H. *et al.* Ultra-fast photonic crystal/quantum dot all-optical switch for future photonic networks. *Opt. Express* **12,** 6606–6614 (2004).
79. Camargo, E. A., Chong, H. M. & De la Rue, R. M. 2D photonic crystal thermo-optic switch based on AlGaAs/GaAs epitaxial structure. *Opt. Express* **12,** 588–592 (2004).
80. Raineri, F. *et al.* Optical amplification in two-dimensional photonic crystals. *Appl. Phys. Lett.* **86,** 091111 (2005).
81. Chu, T., Yamada, H., Ishida, S. & Arakawa, Y. Thermooptic switch based on photonic-crystal line-defect waveguides. *IEEE Photon. Technol. Lett.* **17,** 2083–2085 (2005).
82. Oda, H. & Inoue, K. Observation of Raman scattering in GaAs photonic-crystal slab waveguides. *Opt. Express* **14,** 6659–6667 (2006).
83. Mizuta, E., Watanabe, H. & Baba, T. All semiconductor low-Δ photonic crystal waveguide for semiconductor optical amplifier. *Jpn J. Appl. Phys.* **45,** 6116–6120 (2006).
84. Mingaleev, S. F., Miroshnichenko, A. E. & Kivshar, Y. S. Low-threshold bistability of slow light in photonic-crystal waveguides. *Opt. Express* **15,** 12380–12385 (2007).
85. Hirano, G. & Koyama, F. Slowing light in Bragg reflector waveguide with tilt coupling scheme. *Tech. Dig. IEEE/LEOS Annual Meet.* 86–87 (Orlando, IEEE/LEOS, 2007).
86. Saleh, B. E. A., Teich, M. C. *Fundamentals of Photonics* 2nd edn (Wiley, New Jersey, 2007).
87. Liu, C., Dutton, Z., Behroozi, C. H. & Hau, L. V. Observation of coherent optical information storage in an atomic medium using halted light pulses. *Nature* **409,** 490–493 (2001).
88. Julsgaard, B., Sherson, J., Cirac, J. I., Fiurásek, J. & Polzik, E. S. Experimental demonstration of quantum memory for light. *Nature* **432,** 482–486 (2004).
89. Longdell, J. J., Fraval, E., Sellars, M. J. & Manson, N. B. Stopped light with storage times greater than one second using electromagnetically induced transparency in a solid. *Phys. Rev. Lett.* **95,** 063601 (2005).
90. Sakai, A., Hara, G. & Baba, T. Propagation characteristics of ultra-high Δ optical waveguide on silicon-on-insulator substrate. *Jpn J. Appl. Phys.* **40,** 383–385 (2001).

91. *Silicon Photonics: An Introduction* (eds Reed, G. T. & Knight, A. P.) (Wiley, New Jersey, 2004).
92. *Optical Interconnects The Silicon Approach* (eds Pavesi, L. & Guillot, G.) (Springer, Berlin, 2006).
93. Dulkeith, E., Xia, F., Schares, L., Green, W. M. J. & Vlasov, Y. A. Group index and group velocity dispersion in silicon-on-insulator photonic wires. *Opt. Express* **14,** 3853–3863 (2006).
94. Yamada, K. *et al.* Singlemode lightwave transmission in SOI-type photonic-crystal line-defect waveguides with phase-shifted holes. *Electron. Lett.* **38,** 74–75 (2002).
95. Watanabe, Y. *et al.* Broadband waveguide intersection with low-crosstalk in two-dimensional photonic crystal circuits by sing topology optimization. *Opt. Express* **14,** 9502–9507 (2006).
96. Ishii, S., Nozaki, K. & Baba, T. Photonic molecules in photonic crystal. *Jpn J. Appl. Phys.* **45,** 6108–6111 (2006).
97. Nakagawa, A., Ishii, S. & Baba, T. Photonic molecule lasers composed of GaInAsP microdisks. *Appl. Phys. Lett.* **86,** 041112 (2005).
98. Ishii, S. & Baba, T. Bistable lasing in twin microdisk photonic molecule. *Appl. Phys. Lett.* **87,** 181102 (2005).
99. Astratov, V. N., Franchak, J. P. & Ashili, S. P. Optical coupling and transport phenomena in chains of spherical dielectric microresonators with size disorder. *Appl. Phys. Lett.* **85,** 5508–5510 (2004).
100. Möller, B. M., Woggon, U. & Artemyev, M. V. Coupled-resonator optical waveguides doped with nanocrystals. *Opt. Lett.* **30,** 2116–2118 (2005).
101. Hara, Y., Mukaiyama, T., Takeda, K. & Kuwata-Gonokami, M. Heavy photon states in photonic chains of resonantly coupled cavities with supermonodispersive microspheres. *Phys. Rev. Lett.* **94,** 203905 (2005).
102. Tanabe, T. *et al.* Fast all-optical switching using ion-implanted silicon photonic crystal nanocavities. *Appl. Phys. Lett.* **90,** 031115 (2007).
103. Smith, D. D., Chang, H., Fuller, K. A., Rosenberger, A. T. & Boyd R. W. Coupled-resonator-induced transparency. *Phys. Rev. A* **69,** 063804 (2004).
104. Xu, Q. *et al.* Experimental realization of an on-chip all-optical analogue to electromagnetically induced transparency. *Phys. Rev. Lett.* **96,** 123901 (2006).
105. Suematsu, Y. & Furuya, K. Propagation mode and scattering loss of a two-dimensional dielectric waveguide with gradual distribution of refractive index. *IEEE Trans. Microwave Theory Tech.* **MTT-20,** 524–531 (1972).
106. Lee, K. K., Lim, D. R., Kimerling, L. C., Shin, J. & Cerrina, F. Fabrication of ultralow-loss Si/SiO_2 waveguide by roughness reduction. *Opt. Lett.* **26,** 1888–1890 (2001).
107. Yamada, K. *et al.* Microphotonics devices based on silicon wire waveguiding system. *IEICE Trans. Electron.* **E87-C,** 351–358 (2004).
108. Vlasov, Y. A. & McNab, S. J. Losses in single-mode silicon-on-insulator strip waveguides and bends. *Opt. Express* **12,** 1622–1631 (2004).
109. Tsang, H. K. *et al.* Optical dispersion, TPA and SPM in Si waveguides at 1.5 μm wavelength. *Appl. Phys. Lett.* **80,** 416–418 (2002).
110. Rieger, G. W., Virk, K. S. & Young, J. F. Nonlinear propagation of ultrafast 1.5 μm pulses in high-index contrast silicon-on-insulator waveguides. *Appl. Phys. Lett.* **84,** 900–902 (2004).
111. Yamada, H. *et al.* Nonlinear-optic silicon-nanowire waveguides. *Jpn J. Appl. Phys.* **44,** 6541–6545 (2005).
112. Dulkeith, E., Vlasov, Y. A., Chen, X., Panoiu, N. C. & Osgood Jr, R. M. Self-phase-modulation in submicron silicon-on-insulator photonic wires. *Opt. Express* **14,** 5524–5534 (2006).
113. Oda, H. *et al.* Self-phase modulation in photonic-crystal-slab line-defect waveguides. *Appl. Phys. Lett.* **90,** 231102 (2007).
114. Vlasov, Y. A. & McNab, S. J. Coupling into the slow light mode in slab-type photonic crystal waveguides. *Opt. Lett.* **31,** 50–52 (2006).
115. de Sterke, C. M. *et al.* Efficient slow light coupling into photonic crystals. *Opt. Express* **15,** 10984–10990 (2007).
116. Ozaki, N. *et al.* High transmission recovery of slow light in a photonic crystal waveguide using a hetero group velocity waveguide. *Opt. Express* **15,** 7974–7983 (2007).
117. Yang, L. *et al.* Topology optimisation of slow light coupling to photonic crystal waveguides. *Electron. Lett.* **43,** 923–924 (2007).
118. Meier, M. *et al.* Laser action from two-dimensional distributed feedback in photonic crystals. *Appl. Phys. Lett.* **74,** 7–9 (1999).
119. Sakoda, K., Ohtaka, K. & Ueta, T. Low-threshold laser oscillation due to group-velocity anomaly peculiar to two- and three-dimensional photonic crystals. *Opt. Express* **4,** 481–489 (1999).
120. Noda, S., Yokoyama, M., Imada, M., Chutinan, A. & Mochizuki, M. Polarization mode control of two-dimensional photonic crystal laser by unit cell structure design. *Science* **293,** 1123–1125 (2001).
121. Notomi, M., Suzuki, H. & Tamamura, T. Directional lasing oscillation of two-dimensional organic photonic crystal lasers at several photonic band gaps. *Appl. Phys. Lett.* **78,** 1325–1327 (2001).
122. Altug, H. & Vuckovic, J. Experimental demonstration of the slow group velocity of light in two-dimensional coupled photonic crystal microcavity arrays. *Appl. Phys. Lett.* **86,** 111102 (2005).
123. Sugitatsu, A. & Noda, S. Room temperature operation of 2D photonic crystal slab defect-waveguide laser with optical pump. *Electron. Lett.* **39,** 213–215 (2003).
124. Kiyota, K., Kise, T., Yokouchi, N., Ide, T. & Baba, T. Various low group velocity effects in photonic crystal line defect waveguides and their demonstration by laser oscillation. *Appl. Phys. Lett.* **88,** 201904 (2006).
125. Watanabe, H. & Baba, T. High-efficiency photonic crystal microlaser integrated with a passive waveguide. *Opt. Express* **16,** 2694–2698 (2008).
126. Clap, R., Dimitropoulos, D., Raghunathan, V., Han, Y. & Jalali, B. Observation of stimulated Raman amplification in silicon waveguides. *Opt. Express* **11,** 1731–1739 (2003).
127. Espinola, R. L., Dadap, J. I., Osgood Jr, R. M., McNab, S. J. & Vlasov, Y. A. Raman amplification in ultrasmall silicon-on-insulator wire waveguides. *Opt. Express* **12,** 3713–3718 (2004).
128. Xu, Q., Almeida, R. & Lipson, M. Demonstration of high Raman gain in a submicrometer-size silicon-on-insulator waveguide. *Opt. Lett.* **30,** 35–37 (2005).
129. Espinola, R. J., Dadap, J. I., Osgood, Jr, R. M., McNab, S. J. & Vlasov, Y. A. C-band wavelength conversion in silicon photonic wire waveguides. *Opt. Express* **13,** 4341–4349 (2005).
130. Fukuda, H. *et al.* Four-wave mixing in silicon wire waveguides. *Opt. Express* **13,** 4629–4637 (2005).
131. Okawachi, Y. *et al.* All-optical slow-light on a photonic chip. *Opt. Express* **14,** 2317–2322 (2006).